RESEARCH ARTICLE

Global Change Biology WILEY

Ocean climate and hydrodynamics drive decadal shifts in Northeast Atlantic dinoflagellates

Loïck Kléparski[1,2] ◉ | Grégory Beaugrand[1] ◉ | Clare Ostle[2] ◉ | Martin Edwards[3,4] ◉ | Morten D. Skogen[5] ◉ | Nicolas Djeghri[2] ◉ | Hjálmar Hátún[6] ◉

[1]UMR 8187—LOG—Laboratoire d'Océanologie et de Géosciences, Univ. Littoral Côte d'Opale, CNRS, Univ. Lille, Wimereux, France

[2]Continuous Plankton Recorder Survey, Marine Biological Association, Plymouth, UK

[3]Plymouth Marine Laboratory, Plymouth, UK

[4]School of Biological and Marine Sciences, University of Plymouth, Plymouth, UK

[5]Institute of Marine Research, Bergen, Norway

[6]Faroe Marine Research Institute, Tórshavn, Faroe Islands

Correspondence
Loïck Kléparski, UMR 8187—LOG—Laboratoire d'Océanologie et de Géosciences, Univ. Littoral Côte d'Opale, CNRS, Univ. Lille, 62930 Wimereux, France.
Email: loick.kleparski@hotmail.fr

Abstract

The abundance of large marine dinoflagellates has declined in the North Sea since 1958. Although hypotheses have been proposed to explain this diminution (increasing temperature and wind), the mechanisms behind this pattern have thus far remained elusive. In this article, we study the long-term changes in dinoflagellate biomass and biodiversity in relation to hydro-climatic conditions and circulation within the North Atlantic. Our results show that the decline in biomass has paralleled an increase in biodiversity caused by a temperature-induced northward movement of subtropical taxa along the European shelf-edge, and facilitated by changes in oceanic circulation (subpolar gyre contraction). However, major changes in North Atlantic hydrodynamics in the 2010s (subpolar gyre expansion and low-salinity anomaly) stopped this movement, which triggered a biodiversity collapse in the North Sea. Further, North Sea dinoflagellate biomass remained low because of warming. Our results, therefore, reveal that regional climate warming and changes in oceanic circulation strongly influenced shifts in dinoflagellate biomass and biodiversity.

KEYWORDS
biodiversity change, biomass decline, climate change, dinoflagellate, hydrodynamics, northward movement, subpolar gyre

1 | INTRODUCTION

Climate warming is now affecting marine ecosystems everywhere around the world (IPCC, 2019). In the Northeast Atlantic, important changes have been documented in phytoplankton phenology (i.e. seasonal cycle) and abundance, with a shift in mean annual abundance from a system dominated by dinoflagellates (unicellular mixotrophic phytoplankton) to a system dominated by diatoms (unicellular autotrophic phytoplankton) (Chivers et al., 2020; Djeghri et al., 2023; Hinder et al., 2012). Shift in taxa dominance is thought to have been caused by increasing temperature and wind-induced turbulence, which altered water column stratification (Hinder et al., 2012). This conclusion is based on the assumption that dinoflagellates mainly occur in stratified low-nutrient waters, while diatoms mostly occur in turbulent high-nutrient waters (Kemp & Villareal, 2018; Margalef, 1978; Tréguer et al., 2018). However, this framework is now known to be too conservative, both diatoms and dinoflagellates being found in a large range of habitats, from onshore high-nutrient waters to tropical oligotrophic gyres (Kemp & Villareal, 2018; Malviya et al., 2016; Smayda & Reynolds, 2003).

The biological and ecological shifts that occurred in the Northeast Atlantic region (and especially in the North Sea) over the last 60 years have been frequently attributed to large-scale hydro-climatic variability such as North Atlantic Oscillation (NAO), Atlantic Multidecadal Oscillation (AMO) and Northern Hemisphere Temperature (NHT) anomalies (Beaugrand, 2004; Beaugrand et al., 2014, 2021; Edwards et al., 2001, 2013, 2022). Oceanic inflow has also been identified as a key determinant of plankton community composition in the North Sea (Edwards et al., 2002; Gao et al., 2021; Leterme et al., 2008; Reid et al., 2003). The influxes of water, as well as the biogeochemical and biological properties of this area, are likely related to the strength of the subpolar gyre, a large body of cold rotating low saline waters in the central North Atlantic, which controls the amount of cold fresh subpolar and warm-haline subtropical waters that enter into the North Sea through the Rockall Trough (a deep area west of the British Isles; Figure 1a) (Hátún et al., 2005; Koul et al., 2019). The dynamic hydro-climatic conditions, quantified by the subpolar gyre index (Hátún et al., 2005), can influence the whole Northeast Atlantic ecosystem (Hátún et al., 2009).

In this article, we investigate the long-term changes in dinoflagellate biomass and biodiversity in the Northeast Atlantic, with a regional focus on the North Sea (Figure 1a). We show that the previously documented decline has paralleled an increase in biodiversity caused by the arrival of warm-temperate/haline taxa. We demonstrate that this increase is correlated with climate warming and changes in both hydro-climatic conditions and oceanic circulation. Finally, we show that a strengthening of the subpolar gyre during the 2010s, associated with a major salinity anomaly that appeared in the Northeast Atlantic and an eastward shift of the subpolar front, blocked the northward advection of the warm-temperate/haline taxa along the European shelf-edge, leading to the collapse of dinoflagellate biodiversity in the North Sea. This event thus demonstrates
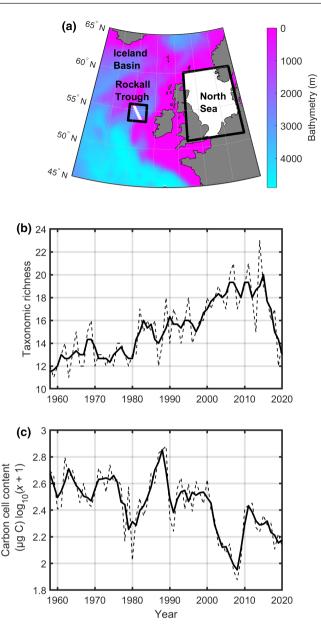

FIGURE 1 Location of the studied areas and long-term changes in dinoflagellate taxonomic richness and biomass in the North Sea. (a) Location of the studied areas. Black squares highlight the Rockall Trough (left) and the North Sea (right). Blank areas display the area where mean annual/monthly taxonomic richness and biomass of dinoflagellates, as well as temperature and salinity, were assessed in the North Sea. In the Rockall Trough, salinity and temperature were assessed along a transect (white line). Colours denote the bathymetry across the Northeast Atlantic. Long-term changes in dinoflagellate taxonomic richness (b) and biomass (c) in the North Sea. The dashed and bold lines display the unsmoothed and the smoothed (by means of a first-order simple moving average, that is a 3-year smoothing window) long-term changes, respectively. Biomass corresponds to a mean per Continuous Plankton Recorder sample.

that climate warming interacts with changes in hydro-climatic conditions and oceanic circulation to alter plankton community composition. Our results therefore emphasise that modelling studies that

simply consider changing biogeographical ranges (thermal niches) in relation to climate warming in isolation are not adequate to project future phytoplankton changes.

2 | MATERIALS AND METHODS

2.1 | Biological data

The Continuous Plankton Recorder (CPR) survey is a long-term plankton monitoring programme that has sampled plankton on a monthly basis in the North Atlantic Ocean and its adjacent seas since 1958. The sampling mechanism is a high-speed plankton recorder towed behind voluntary merchant ships called 'ships of opportunity' at a depth of approximately ~7–10m (Batten et al., 2003; Warner & Hays, 1994). Here we used the abundance data collected for the dinoflagellates in the North Atlantic Ocean, with an emphasis on the Northeast Atlantic regions (34°N to 65°N, −27°E to 17°E) and the North Sea (51°N to 60°N, −3°E to 9°E) between 1958 and 2020 (Figure 1a; Text S1). Each value of abundance corresponds to a number of cells per CPR sample, which corresponds to ~3m^3 of seawater filtered (Jonas et al., 2004). Note that the physiological states of the collected organisms cannot be assessed during sample processing. Taxa abundances were converted into biomass by multiplying them with the corresponding mean cell size (i.e. carbon cell contents), which originate from the database compiled by Barton and colleagues (Barton et al., 2013). Only two taxa were not found, even after looking for updated or synonym names (i.e. *Protoceratium reticulatum* and *Exuviaella* spp.). Therefore, a total of 49 taxa (the ones for which a mean cell size was available) was used in the analyses. We warn that mean cell size was assumed to be constant, although it has been shown that intra-specific variations in size and seasonal morphological plasticity can be important for some phytoplanktonic taxa (Ligowski et al., 2012).

2.2 | Environmental gridded data

Monthly sea surface temperature (SST, °C) and sea surface salinity (SSS, PSU) originated from the Ocean Reanalysis System 5 (ORAS5) dataset and were downloaded from the Copernicus climate data store (https://cds.climate.copernicus.eu/cdsapp#!/dataset/reanalysis-oras5?tab=overview). Wind components (U and V, zonal and meridional components of the wind at 10m above the surface, respectively) and total precipitation (mm) above the North Sea originated from the ERA5 dataset and were also downloaded from the Copernicus climate data store (https://cds.climate.copernicus.eu/cdsapp#!/dataset/reanalysis-era5-single-levels-monthly-means?tab=overview). Mean annual SST, SSS, U and V wind and total precipitation were estimated at the North Sea scale (51°N to 60°N, 3°W to 9°E; Figures 1a and 6d; Figure S9b–d) and across the Rockall Trough (only for SST and SSS; 54°N to 55.5°N, 15.25°W to 13.25°W; Figures 1a and 6c). Annual SST and SSS anomalies were estimated

for each year between 2003 and 2020, based on the means between 1965 and 1975 (which is a period of relative stability in the state of various hydro-climatic indices at the North Atlantic scale; see Figure 6), for the region from 36°N to 64°N and from −25°E to 15°E, to characterise the cold and fresh anomalies that have been reported in the North Atlantic during the mid-2010s (Figures S10 and S11) (Desbruyères et al., 2021; Holliday et al., 2020; Josey et al., 2018).
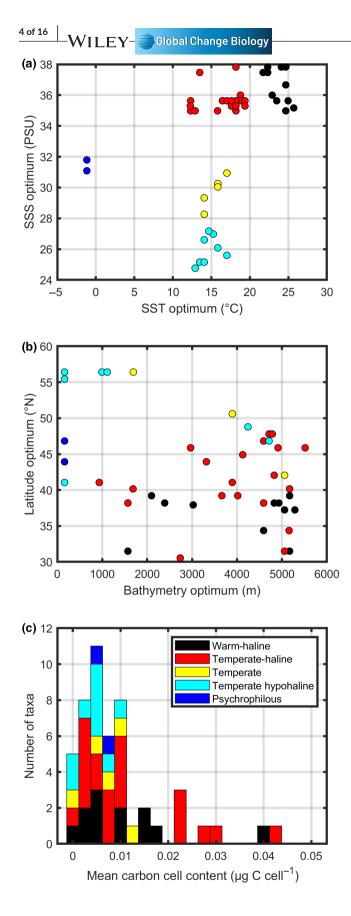
Bathymetry (m) originated from the GEBCO Bathymetric Compilation Group 2019 (Figures 1a and 2b) (the GEBCO_2019 Grid—a continuous terrain model of the global oceans and land). Data were provided by the British Oceanographic Data Centre, National Oceanography Centre, NERC, UK. https://doi.org/10.5285/836f016a-33be-6ddc-e053-6c86abc0788e. (https://www.bodc.ac.uk/data/published_data_library/catalogue/10.5285/836f016a-33be-6ddc-e053-6c86abc0788e/). All data were interpolated on a regular 0.25° grid, if not already provided on such a grid.

2.3 | Other hydro-meteorological/hydro-climatic data and indices

Data on North Sea inflow originated from the NORWECOM model, which has been validated against observations from the North Sea (see Text S1). In the present study, the model was used with a horizontal resolution of 10×10 km^2, and 20 bottom-following sigma layers in the vertical, in an area covering an extended North Sea. For more details on the model set-up, see Hjøllo et al. (2009; Text S1). The model was run for the period 1958–2021 with a 5-year spin-up. Model data were stored as monthly means, and the water transports into the North Sea were computed from the monthly mean velocity fields across a transect from Orkney to Utsira (along 59.17°N and from −2.30°E to 5.15°E). Positive direction is northwards; therefore, inflow appears as a negative number. All numbers are given in Sverdrup (1Sv = 10^{6}m^{3}s^{-1}). The data were finally averaged at a yearly scale (Figure S9a).

Salinity time series for the Fair Isle Current Water (Figure S9e; Text S1), that is waters entering through the northwest North Sea and originating from the Atlantic Ocean, were provided by Marine Scotland Science, Aberdeen, United Kingdom. Data were downloaded at https://ocean.ices.dk/core/iroc.

The North Atlantic subpolar gyre index (Figure 6a) was assessed by means of an Empirical Orthogonal Function (EOF, also called principal component analysis) analysis of the sea surface height (SSH) over the North Atlantic subpolar and subtropical gyres (from 30°N to 65°N and 80°W to 0°E). SSH data came from the DUACS DT2014 altimetry data and cover the time period 1994–2020. The subpolar gyre index summarises the strength and the extent of the subpolar gyre, that is when the index is positive, it indicates a weak subpolar gyre (so more subtropical waters are passing along the European shelf-edge) and inversely, when the index is negative, it indicates a strong subpolar gyre (so more subpolar waters are being advected along the European shelf-edge) (Hátún et al., 2005; Hátún & Chafik, 2018; Koul et al., 2019).

FIGURE 2 Ecological characteristics of the five taxonomic assemblages. (a) Relationships between the optimums for sea surface salinity (SSS) and sea surface temperature (SST) of the 49 dinoflagellates. (b) Relationships between the latitude and bathymetry optimums of the 49 dinoflagellates. (c) Distribution of the mean carbon cell contents ($\mu g\,C\,cell^{-1}$) among the five assemblages identified by means of a cluster analysis (see Section 2). In (a–c), colours enable the distinction of the five assemblages: the warm-haline assemblage is in black, the temperate-haline in red, the temperate in yellow, the temperate hypohaline in pale blue and the psychrophilous in dark blue. Some taxa have identical/close environmental optimums; therefore, the number of dots in each panel is not always equal to 49.

& Deser, 2010). Based on the sea surface level pressure difference between the Azores and Iceland, a negative index reflects lower than usual westerly winds in the Northeast Atlantic (i.e. colder and drier conditions), whereas a positive index means higher than usual westerly winds (i.e. warmer and wetter meteorological conditions in the Northeast Atlantic). Although observed for all months of the year, the NAO is stronger in the winter. Monthly NAO indices were averaged at a yearly scale and smoothed by means of a first-order simple moving average (i.e. smoothing window of 3 years) to highlight persistent phases.

The AMO (Figure 6b) index was provided by the NOAA physical science laboratory and was downloaded at http://www.psl.noaa.gov/data/timeseries/AMO/. The AMO index reflects the low-frequency variability in the North Atlantic Ocean and is calculated from the unsmoothed and detrended Kaplan SST V2 dataset (Text S1). However, it has been recently suggested that the AMO is not a natural oscillation but instead results from external forces (e.g. volcanism, aerosol accumulation and human-induced climate change) (Mann et al., 2021). Nevertheless, the variability represented by the AMO-like pattern (also called Atlantic Multidecadal Variability or AMV) has been related with many different physical and biological changes in the North Atlantic Ocean (Beaugrand et al., 2021; Edwards et al., 2013, 2022; Faillettaz et al., 2019). Monthly AMO indices were averaged at an annual scale.

NHT (Figure 6b) anomalies originated from the NASA Goddard Institute for Space Studies (GISS) and were downloaded at https://data.giss.nasa.gov/gistemp/. The index corresponds to the combined land-surface air and sea-surface temperature anomalies at the scale of the Northern Hemisphere based on the reference period 1951–1980 (Text S1). Monthly NHT anomalies were average at an annual scale.

2.4 | Long-term changes in North Sea dinoflagellate biomass and biodiversity

Dinoflagellate biodiversity (measured as taxonomic richness) was quantified for each year in the North Sea (Figure 1a) between 1958 and 2020 by considering the total number of taxa with a positive biomass in at least one CPR sample. The biomass of the 49 taxa in each CPR sample was subsequently added, and the resulting total biomass was interpolated in the North Sea on a regular 1°×1° grid for each

The NAO (Figure 6a) index was downloaded from the National Centers for Environmental Information (NCEI) at https://www.ncei.noaa.gov/access/monitoring/nao/. The NAO is an important source of hydro-meteorological variability in the Northeast Atlantic (Hurrell

month between 1958 and 2020, averaged at an annual scale and finally transformed with a $\log_{10}(x+1)$ function to account for the large variability in biomass and avoid negative values (biomass range from 0 to more than 8000 µg C per CPR sample). A larger grid resolution was chosen here (i.e. 1°×1° instead of 0.25°×0.25° for environmental data) because of the nature of the CPR sampling, which is carried out at a monthly scale over large areas and is also heterogeneous in space and time (Richardson et al., 2006). Furthermore, the CPR uses a 270 µm mesh silk that mostly samples large armoured formalin-preservable dinoflagellates and undersamples smaller fragile phytoplanktonic taxa. Nevertheless, the CPR collects an important fraction of the abundance of each taxon and is therefore robust to examine interannual and seasonal patterns (Richardson et al., 2006). A shift towards larger cell size is very unlikely to have affected the sampling by the CPR because a shift towards smaller cell is usually observed in the context of warming because of an enhanced grazing by the larger taxa (Lewandowska & Sommer, 2010).

Long-term changes in annual taxonomic richness and total biomass were finally smoothed by means of a first-order (i.e. smoothing window of 3 years) simple moving average (Figure 1b,c). The Pearson correlation coefficient was calculated between the unsmoothed taxonomic richness and total biomass. Probabilities were calculated with correction after accounting for temporal autocorrelation (p_{ACF}) by adjusting the degree of freedom (df_{ACF}) following the method used in Beaugrand and Reid (Beaugrand & Reid, 2012). However, as strong autocorrelation sometimes results in an extreme reduction in the degree of freedom, correlations might be non-significant at the usual threshold of .05. Therefore, correlations were considered significant at the threshold of .15 if they explained more than 40% of the total variance, a method that has already been applied elsewhere (Beaugrand & Reid, 2012; Luczak et al., 2011); see the discussion in Beaugrand and Reid (2012) and references therein for further details. Significant correlations at the usual threshold level of .05, but explaining less than 40%, were also considered.

To assess whether annual taxonomic richness was affected by the changes in CPR sampling effort, taxonomic richness was re-estimated by randomly selecting a constant number of CPR samples each year (i.e. 569 samples, the minimal number of samples collected during the year 1978). The operation was repeated 10,000 times, and the resulting simulated taxonomic richness was averaged. Pearson correlation coefficients were finally estimated between the changes in annual taxonomic richness and the annual number of CPR samples collected in the North Sea and between the changes in annual taxonomic richness and the changes in mean annual simulated taxonomic richness (under a constant sampling effort), with the same correction to account for temporal autocorrelation as mentioned above (Figure S1).

2.5 | Environmental optimum

The environmental optimum (for SSS, SST, latitude and bathymetry) was characterised for the 49 dinoflagellates by applying the technique of the species chromatogram (Kléparski & Beaugrand, 2022). SST and SSS were used because distinct phytoplankton assemblages are associated with distinct water masses (Fehling et al., 2012). Furthermore, temperature has a strong influence on ectotherm growth rate and has been identified as a key driver explaining global patterns in phytoplankton diversity distribution (Martin & Huey, 2008; Righetti et al., 2019; Thomas et al., 2012).

The species chromatogram method is based on the ecological niche concept developed by G. E. Hutchinson, who defined the niche of a species as the set of environmental conditions enabling a species to grow, maintain and reproduce (Hutchinson, 1957). Usually, this niche concept is assimilated to a p-dimensional hypervolume where p represents various environmental variables (e.g. SST, SSS). The species chromatogram method has been recently developed to (i) display the multidimensional ecological niche of a species into a two-dimensional space and (ii) characterise niche optimum along each environmental dimension, assuming that the highest abundance or biomass reflects optimal environmental conditions (Brown, 1984; Kléparski & Beaugrand, 2022).

First, values of SSS, SST and bathymetry were attributed to each CPR sample collected in the North Atlantic Ocean between 1958 and 2020 by means of nearest-neighbour interpolation, except latitude, which was already documented in the CPR database. Second, changes in each taxa biomass were represented along four environmental gradients (one for each environmental variable) divided into α equidistant categories (here $\alpha=50$ categories). In each category, the mean taxa biomass was estimated by considering $k\%$ of the CPR samples with the highest biomass (here $k=100\%$) if at least m samples were present in that category (here $m=1$ sample). Third, the mean biomass along each dimension were standardised between 0 and 1 and then smoothed by means of a second-order moving average. The environmental optimums were finally assessed along each dimension by identifying the category where the highest biomass was detected. Tests performed with $\alpha=25$ and $\alpha=75$ showed that the number of categories did not substantially influence our estimations of environmental optimums (Table S1, see however *Ceratium gibberum* or *C. teres*) of most taxa.

2.6 | Taxonomic assemblage

The 49 dinoflagellates were decomposed into taxonomic assemblages based on their standardised environmental optimums for SSS and SST. Each value of the resulting matrix $\mathbf{T}_{49,2}$ (49 taxa by 2 environmental variables) was standardised between 0 and 1. To do so, the following transformation was applied for all t values in each column of $\mathbf{T}$:

$$t^*_{(i,p)} = \frac{t_{(i,p)} - \min(t_p)}{\max(t_p) - \min(t_p)} \tag{1}$$

with $t^*_{(i,p)}$ the standardised optimum for the taxa i along the environmental variables p (here $i=49$ taxa and $p=2$ environmental variables, i.e. SST and SSS) and $\min(t_p)$ and $\max(t_p)$ the minimum and maximum, respectively, along dimension p (Legendre & Legendre, 1998).

An Euclidean square distance matrix $\mathbf{D}_{49,49}$ was then calculated between the 49 taxa based on $\mathbf{T}^*_{49,2}$. The Euclidean distance among two taxa was calculated as follows (Legendre & Legendre, 1998):

$$D\left(\text{species}_i, \text{species}_j\right) = \sqrt{\sum_{k=1}^{p} \left(t^*_{i,k} - t^*_{j,k}\right)^2} \tag{2}$$

Finally, a cluster analysis based on the complete linkage method was applied, and five assemblages were identified at the cut-off level of 1.7 (Figure 2; Figure S2). The cut-off level was chosen to select a maximum number of groups and to limit the number of assemblages with a low number of taxa. The mean long-term annual and monthly changes in taxonomic richness and biomass were then estimated for each assemblage in the North Sea following the method previously used for assessing the total dinoflagellate biomass and taxonomic richness in the North Sea (Figure 3). Trends in monthly biomass were assessed by means of linear least-squares regression (Figure 4; Figures S3–S7) (Legendre & Legendre, 1998).

2.7 | Long-term changes in the taxonomic richness and biomass of each assemblage at the scale of the Northeast Atlantic

Taxonomic richness and biomass were interpolated on a regular $1° \times 1°$ grid for each year and every 2-month period between 1958 and 2020 at the scale of the Northeast Atlantic (34°N to 65°N, 27°W to 17°E). A 2-month period was considered here to account for the spatio-temporal variability in the CPR sampling (i.e. the sampling effort is higher in the North Sea than in the rest of the Northeast Atlantic region) (Richardson et al., 2006). Maximum taxonomic richness and biomass were then assessed (instead of the mean, which would have been affected by the large number of low/null values caused by the spatio-temporal variability in the CPR sampling) in each geographical cell by considering all years and months for four temporal periods corresponding to persistent negative or positive smoothed NAO phases (Figure 6a): (i) 1958–1971 (persistent negative NAO), (ii) 1972–1995 (persistent positive NAO), (iii) 1996–2012 (persistent negative NAO) and (iv) 2013–2020 (persistent positive NAO). Each period is therefore of unequal length (i.e. 14, 24, 17 and 8 years, respectively). The resulting maps were finally smoothed by means of two successive spatial second-order weighted moving average (weighted by the inverse of the squared number of geographical cells; Figures 5; Figure S8). Maps of maximum taxonomic richness were standardised by means of Equation (1) (Figure S8), and maps of maximum biomass were transformed with a $\log_{10}(x+1)$ function (Figure 5).

2.8 | Relationships between long-term changes in biomass, taxonomic richness and hydro-climatic variability

Pearson correlation coefficients were calculated between (unsmoothed) mean long-term changes in biomass ($\log_{10}(x+1)$ transformed), taxonomic richness and various hydro-climatic indices (i.e. NHT, AMO, NAO, subpolar gyre index, inflow into the North Sea, mean annual SST and SSS in the North Sea and the Rockall Trough (see Figure 1a) and North Sea U and V winds; Tables S2 and S3) with the same correction as previously used to account for temporal autocorrelation (see above).

3 | RESULTS

3.1 | Changes in North Sea dinoflagellates

Long-term changes in the biomass and biodiversity (i.e. taxonomic richness) of planktonic dinoflagellates were first examined in the North Sea (Figure 1a). To do so, the abundance data of 49 taxa collected by the CPR survey between 1958 and 2020 were converted into (i) biomass based on taxa mean cell size (Barton et al., 2013) and (ii) taxonomic richness as a measure of biodiversity. Results showed that taxonomic richness in this region has doubled since 1958, from ~10 to more than 20 taxa during the 2000s (Figure 1b). The increase was almost linear, but in the mid-2010s, a strong and rapid decline was observed from 23 taxa in 2014 to 12 and 14 in 2019 and 2020, respectively (Figure 1b). The taxa that were recorded in 2014 but not in 2019 were *Ceratium. arcticum*, *C. arietinum*, *C. bucephalum*, *C. carriense*, *C. compressum*, *C. declinatum*, *C. hexacanthum*, *C. massiliense*, *Pyrophacus* spp., *Podolampas* spp. and *Pronoctiluca pelagica*. No changes occurred in the number of recorded taxa during that period (Figure S1a). Although a significant correlation was found between the changes in taxonomic richness and the number of CPR samples collected in the North Sea (Figure S1b), changes in mean simulated taxonomic richness (based on a constant number of CPR samples randomly selected for each year) indicated that the biodiversity trend was not related to the increasing sampling effort (Figure S1b,c). On the other hand, total biomass declined, especially after the 1990s (Figure 1c), and these changes were negatively correlated with the changes in biodiversity ($r = -.43$, $p < .01$ and $p_{ACF} = .12$ before and after correction for autocorrelation, respectively).

3.2 | Decomposition of the dinoflagellate biodiversity into taxonomic assemblages

Distinct phytoplankton assemblages are associated with different water masses (Fehling et al., 2012). Therefore, the 49 dinoflagellates were decomposed into taxonomic assemblages by means of a cluster analysis based on their environmental optimums for SST and salinity (SSS) in the North Atlantic. Five assemblages were identified (Figure 2a; Table S1; Figure S2): (i) a warm-haline assemblage gathering taxa with high optimums for SST and SSS; (ii) a temperate-haline assemblage with medium SST and high SSS optimums; (iii) a temperate assemblage with medium optimums for SST and SSS; (iv) a temperate hypohaline assemblage with low
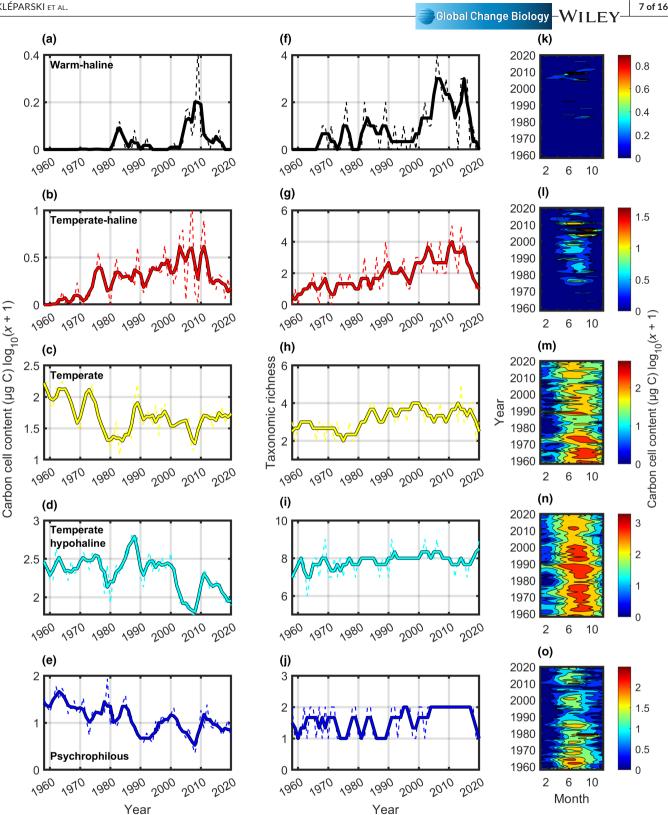
FIGURE 3 Long-term changes in biomass and taxonomic richness of the five assemblages in the North Sea. Long-term changes in the mean annual biomass (per Continuous Plankton Recorder sample) of (a) the warm-haline, (b) the temperate-haline, (c) the temperate, (d) the temperate hypohaline and (e) the psychrophilous assemblage in the North Sea (Figure 1a). Long-term changes in the taxonomic richness of (f) the warm-haline, (g) the temperate-haline, (h) the temperate, (i) the temperate hypohaline and (j) the psychrophilous assemblage in the North Sea (Figure 1a). In (a–j), colours enable distinction of the assemblages (see Figure 2 legend). (k–o) Long-term changes in the mean monthly biomass of (k) the warm-haline, (l) the temperate-haline, (m) the temperate, (n) the temperate hypohaline and (o) the psychrophilous assemblage in the North Sea. Blue and red colours represent low and high biomass, respectively. Each panel has a distinct colour scale. See also Figures S3–S7.
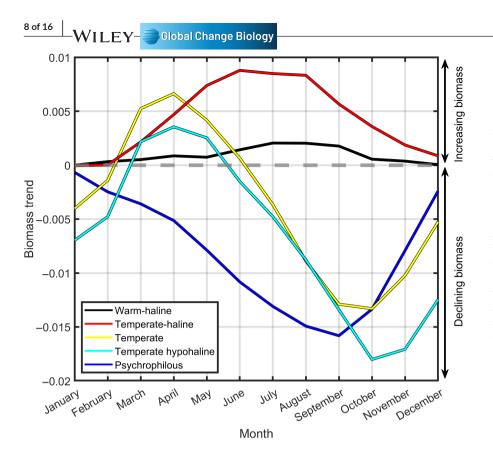
FIGURE 4 Trends in mean monthly biomass for each assemblage between 1958 and 2020 in the North Sea. Positive trends indicate an increasing biomass, while negative trends indicate a declining biomass. The dashed grey line indicates no change in biomass. The warm-haline assemblage is in black, the temperate-haline in red, the temperate in yellow, the temperate hypohaline in pale blue and the psychrophilous in dark blue. A phenological shift from the autumn (i.e. negative biomass trend) to the spring (i.e. positive biomass trend) is visible for the temperate and temperate hypohaline assemblages. The negative trends exhibited by the psychrophilous assemblage indicate that it has reached the limits of its phenological plasticity (Beaugrand & Kirby, 2018).

SSS and medium SST optimums; and (v) a psychrophilous assemblage composed of taxa occurring in cold medium-haline waters. The taxonomic composition of each assemblage is displayed in Table 1. Taxa composing the warm-haline and temperate-haline assemblages also exhibited high and low optimums for bathymetry and latitudes, respectively (Figure 2b), and high variation in cell size (Figure 2c), suggesting that those assemblages mainly occur in low-latitude oceanic waters, thereby subtropical or possibly tropical regions (Smayda & Reynolds, 2003). On the contrary, taxa composing the temperate, the temperate hypohaline and the psychrophilous assemblages had low and high optimums for bathymetry and latitudes, respectively (Figure 2b), associated with smaller mean cell size (Figure 2c), indicating that those assemblages mainly occur over the continental shelves and shelf-edges (Smayda & Reynolds, 2003). (Some taxa of the temperate and temperate hypohaline assemblages were also found over high-latitude oceanic areas; Figure 2b).

3.3 | Long-term changes of the five assemblages in the North Sea

The long-term changes in biomass and taxonomic richness of the five assemblages were subsequently examined in the North Sea (Figure 3). The warm-haline and temperate-haline exhibited an increase in biomass, with two pulses in the 1980s and circa 2009 for the former and a constant increase from the end of the 1960s until the end of the 2000s for the latter (Figure 3a,b). The highest biomass of both assemblages was observed between 2000 and 2011, followed by a collapse

during the 2010s (Figure 3a,b). The temperate assemblage exhibited a decline from the middle of the 1970s to the middle of the 1980s, followed by a period of relative stability (Figure 3c). In contrast, the last assemblages showed a decrease in biomass, with the lowest values being observed at the end of the 2000s (Figure 3d,e). Long-term changes in taxonomic richness exhibited different patterns; the biodiversity of warm-haline and temperate-haline assemblages increased, especially during the 2000s (Figure 3f,g), whereas the biodiversity of the three others only slightly rose (Figure 3h–j). The biodiversity of the five groups, but especially the temperate hypohaline, diminished during the mid-2010s (Figure 3f–j).

The examination of changes in monthly biomass revealed pronounced phenological shifts for most assemblages. The warm-haline and the temperate-haline assemblages were first detected in the North Sea in autumn (during the 1970s and the 1960s, respectively). Then, both assemblages exhibited gradually higher biomass in autumn, then in summer and finally in spring (Figures 3k,l and 4; Figures S3 and S4). On the contrary, the temperate and temperate hypohaline assemblages were initially mostly abundant in autumn and summer and then underwent a decline, associated with an increasing biomass in spring, while the psychrophilous assemblage declined continuously in all months (Figures 3m–o and 4; Figures S5–S7).

To better understand these biological shifts in the North Sea, long-term changes in biomass were investigated in the Northeast Atlantic (Figure 5). Four different periods were chosen based on shifts in persistent (i.e. smoothed) NAO states, which is the principal mode of atmospheric variability in this region (Hurrell & Deser, 2010) (Figure 5). The warm-haline and temperate-haline assemblages exhibited high biomass in the Bay of Biscay, the subtropical gyre and
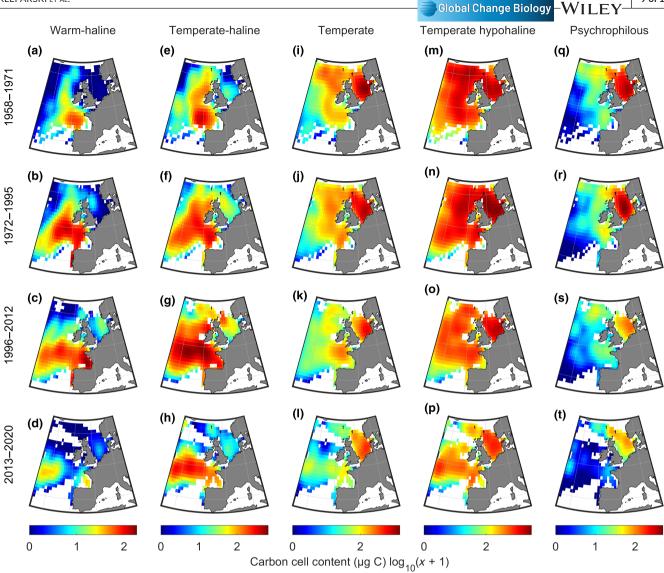
FIGURE 5 Mean long-term changes in maximum biomass of each assemblage from 1958 to 2020. Spatial distribution of the maximum biomass (per Continuous Plankton Recorder sample) of (a–d) the warm-haline, (e–h) the temperate-haline, (i–l) the temperate, (m–p) the temperate hypohaline and (q–t) the psychrophilous assemblage. Spatial distribution of the maximum biomass between (a, e, i, m and q) 1958–1971, (b, f, j, n and r) 1972–1995, (c, g, k, o and s) 1996–2012 and (d, h, l, p and t) 2013–2020. Each chosen time period corresponds to a persistent negative (1958–1971 and 1996–2012) or positive (1972–1995 and 2013–2020) North Atlantic Oscillation phase and is therefore of unequal length. Blue and red colours display low and high maximum biomass, respectively. Missing values are in white. Notice that each assemblage is displayed on a different colour scale.

along the European shelf-edge (Figure 5a–h). Their biomass increased northwards along the European shelf-edge from 1958 to 2012 (Figure 5a–c,e–g), but decreased and retreated during the mid-2010s; this was especially prominent for the warm-haline assemblage (Figure 5d,h). The biomass of both assemblages also increased, first in the northwest and subsequently in the whole North Sea (Figure 5a–h), indicating a colonisation of this area following the path of the North Atlantic Current passing through the Rockall Trough (Figure 1a) and not through the English Channel. Although the temperate assemblage also exhibited high biomass along the European shelf-edge and in the North Sea during 1958–1995, its biomass diminished after, except in the North Sea (Figure 5i–l). On the contrary, the temperate hypohaline assemblage, which was present everywhere north of 45°N, showed

a decline in biomass everywhere, although this group still exhibited the highest observed values (Figure 5m–p). Last, the psychrophilous assemblage occurring in the North Sea decreased continuously (Figure 5q–t). Similar results were observed with taxonomic richness (Figure S8; Text S2). These results thereby reveal that the North Sea changes were related to Northeast Atlantic changes.

3.4 | Relationships between North Sea dinoflagellate shifts and hydro-climatic variability

A correlation analysis was performed to examine the relationships between hydro-climatic variability at both large and regional scales and

TABLE 1 Composition and ecological characteristics of the five taxonomic assemblages. The name of each assemblage is displayed in the first column, number of taxa in the second, taxonomic composition in the third and ecological characteristics (e.g. environmental optimum) in the fourth. Taxa names are those recorded in the Continuous Plankton Recorder database.
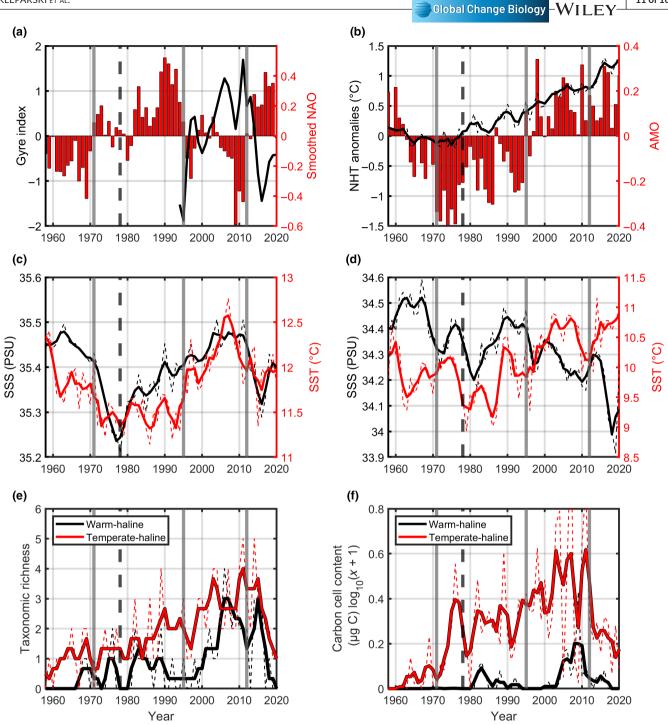
Assemblage name	Number of taxa	Taxonomic composition	Ecological characteristics
Warm-haline	12	*Ceratium kofoidii, Amphisolenia* spp., *Ceratium carriense, Ceratium extensum, Ceratium massiliense, Ceratium pentagonum, Ceratium petersii, Ceratium setaceum, Ceratium trichoceros, Ceratocorys* spp., *Cladopyxis* spp. and *Podolampas* spp.	Low-latitude oceanic taxa with high optimum for sea surface salinity (SSS) and sea surface temperature (SST)
Temperate-haline	21	*Ceratium falcatum, Ceratium arietinum, Ceratium belone, Ceratium buceros, Ceratium candelabrum, Ceratium compressum, Ceratium declinatum, Ceratium gibberum, Ceratium hexacanthum, Ceratium inflatum, Ceratium karstenii, Ceratium lamellicorne, Ceratium platycorne, Ceratium praelongum, Ceratium pulchellum, Ceratium teres, Ceratium vulture, Gonyaulax* spp., *Oxytoxum* spp., *Ceratium falcatiforme* and *Ceratium longirostrum*	Low-latitude oceanic taxa with medium optimum for SST and high optimum for SSS
Temperate	5	*Ceratium macroceros, Ceratium horridum, Pyrophacus* spp., *Ceratium bucephalum* and *Pronoctiluca pelagica*	Pseudo-oceanic taxa with medium optimums for SSS and SST
Temperate hypohaline	9	*Ceratium fusus, Ceratium furca, Ceratium lineatum, Ceratium tripos, Ceratium azoricum, Ceratium minutum, Dinophysis* spp. Total, *Protoperidinium* spp. and *Prorocentrum* spp. Total	Taxa found in the entire Northeast Atlantic region with low optimum for SSS and medium optimum for SST
Psychrophilous	2	*Ceratium longipes* and *Ceratium arcticum*	Subarctic taxa with medium optimum for SSS and low optimum for SST

the long-term changes in North Sea biomass and taxonomic richness. Negative relationships were identified between the biomass of total dinoflagellate and the temperate hypohaline and psychrophilous assemblages and NHT anomalies, AMO and North Sea SST, indicating a negative effect of warming. Significant relationships were also detected between these assemblages and the NAO, including changes in Rockall SST, oceanic inflow, North Sea winds and SSS (Figures 3 and 6; Table S2; Figure S9a–c), suggesting a negative effect of changes in oceanic circulation. On the contrary, positive relationships were observed between temperature and total taxonomic richness, especially with the warm and temperate-haline assemblages (Table S3). The taxonomic richness of the latter was also related with oceanic inflow into the North Sea, while its long-term changes in biomass were positively correlated with the subpolar gyre index (Figure S9a; Tables S2 and S3). Hence, the correlation analysis confirmed results from a previous study, that is dinoflagellate decline was related to increasing SST and winds (Hinder et al., 2012), but they also provide evidence that climate warming and changes in the subpolar gyre, in conjunction, altered dinoflagellate community composition and enabled the arrival of the warm/temperate-haline assemblages in the North Sea.

To confirm this hypothesis, long-term changes in hydro-climatic conditions were compared with long-term changes in North Sea dinoflagellate biomass and biodiversity, based on the four different periods previously defined (bold vertical grey lines in Figure 6). During the first period (1958–1971), the NAO was in a persistent negative phase (i.e. colder and dryer conditions above western Europe, Hurrell & Deser, 2010), while NHT anomalies and the AMO shifted from positive to negative phases, indicating a cooling of both atmospheric and oceanic temperatures (Figure 6a,b). SSS and SST declined in the Rockall Trough and were more variable in the North

Sea (Figures 1a and 6c,d). Therefore, the waters passing through the Rockall Trough were mostly of subpolar origin, although some pulses of subtropical waters also occurred, as indicated by the taxonomic richness of the warm and temperate-haline assemblages that started to increase, an observation confirmed by the presence of these groups along the north-western European shelf-edge (although to a low level; Figures 5a,e and 6e,f). These pulses were made possible because of the large variability in the state of the NAO from 1 month to another and its influence on the gyre circulation (Hurrell & Deser, 2010). The remaining three assemblages also exhibited high biomass during this period (Figures 3c–e and 5i,m,q).

During the second period (1972–1995), the NAO shifted to a persistent positive phase, indicating milder and wetter conditions above western Europe associated with stronger westerly winds (Hurrell & Deser, 2010) (Figure 5a). However, until the end of the 1970s, SST and SSS first strongly declined in both the Rockall Trough and the North Sea, corresponding to the Great Salinity Anomaly (Dickson et al., 1988), an exceptional hydro-climatic event that negatively impacted the biomass of all assemblages (Figure 3a–e). Then, in 1978, the Northern Hemisphere started to warm (shift from negative to positive NHT anomalies; vertical bold dashed line in Figure 6), and more saline (i.e. subtropical) waters were passing through the Rockall Trough, although SST remained low because of the negative AMO phase (Figure 6b,c). SSS also increased in the North Sea, confirming that more subtropical waters were reaching this area (Figure 6d). Biomass and taxonomic richness of the warm and temperate-haline assemblage increased in the North Sea, especially in its northwestern part (Figure 5b,e,f; Figure S8b,f). Oceanic inflow also increased during that period, which may have facilitated the entry of these assemblages into the North Sea (Figure S9a). The taxonomic

FIGURE 6 Relationships between long-term changes in North Sea warm/temperate-haline dinoflagellate biomass and taxonomic richness and some indices of hydro-climatic variability. (a) Long-term changes in the subpolar gyre index (black line) and North Atlantic Oscillation (NAO, smoothed by means of a first-order simple moving average to highlight persistent phases, red bars). Low (high) values of the subpolar gyre index correspond to a strong (weak) subpolar gyre. (b) Long-term changes in Northern Hemisphere Temperature (NHT, black lines) anomalies and Atlantic Multidecadal Oscillation (AMO, not smoothed, red bars). (c, d) Long-term changes in mean annual sea surface salinity (SSS, black lines) and sea surface temperature (SST, red lines) across (c) the Rockall Trough and (d) in the North Sea (Figure 1a). (e, f) Long-term changes in (e) maximum taxonomic richness and (f) mean annual biomass (per Continuous Plankton Recorder sample) of the warm-haline (black lines) and temperate-haline (red lines) assemblages (see Figure 3a,b,f,g). Both assemblages are plotted on the same y-axis (left). In (b–f), the dashed and bold lines display the unsmoothed and the smoothed (by means of a first-order simple moving average, that is a 3-year time window) data, respectively. Vertical bold grey lines highlight the shifts in persistent NAO phases, and vertical bold dashed black lines indicate the year 1978, when NHT anomalies became positive.

richness and biomass of the temperate-haline assemblage were the first to increase because this group has high environmental optimums for SSS but medium for SST (Figure 2a).

During the third period (1995–2012), the NAO shifted to a persistent negative phase, that is colder and dryer conditions above western Europe (Hurrell & Deser, 2010), but the AMO shifted to a positive phase, indicating warming (Edwards et al., 2013) (Figure 6a,b). At the same time, the subpolar gyre index also shifted from negative to positive values, so more warm saline subtropical waters were passing through the Rockall Trough and SST increased in the North Sea (Figure 6a,c,d). The spatial distributions of the warm and temperate-haline assemblages were at their maximum in the Northeast Atlantic (Figure 5c,g; Figure S8c,g), while their North Sea biomass and taxonomic richness reached their highest values, although SSS and oceanic inflow were declining (Figure 6d–f; Figure S9a). On the contrary, the biomass of the three other assemblages were at their minimum, especially by the end of the 2000s, when the lowest persistent negative NAO and highest North Sea SST were observed (Figures 3c–e and 6a,c,d). However, their biomass increased again shortly after that, when a short cooling occurred in both the Rockall Trough and the North Sea, and values close to those of the late 1990s were again observed, but this increase did not persist for the temperate hypohaline and psychrophylous assemblages (Figures 3c,d and 6c,d).

During the last period (2013–2020), the NAO shifted again to a persistent positive phase while the subpolar gyre index shifted to negative values (Figure 6a). Therefore, more subpolar waters passed through the Rockall Trough, where SSS and SST declined (Figures 6c), an event that was associated with the eastward propagation of an exceptional cold fresh anomaly in the Northeast Atlantic (Figures S10 and S11). In the North Sea, the biomass and taxonomic richness of the warm- and temperate-haline assemblages collapsed, while the area was freshened and warmed (Figure 6d–f). No increase in mean precipitation was observed above the North Sea at that time, but an increasing oceanic inflow associated with a freshening of the waters entering through the Fair Isle current (northwest North Sea) were detected, indicating an enhanced inflow of subpolar waters and the arrival of the salinity anomaly in the North Sea (Figure S9a,d,e). Hence, the collapse of those assemblages might be related with changes in subpolar gyre strength and the associated inflow of the salinity anomaly into the North Sea. The other assemblages (except the temperate one) also declined (Figure 3c–e), but as they have medium to low SSS and SST optimums (Figure 2a), they should have been favoured by the advection of subpolar waters, which was shortly observed circa 2010 when the biomass of both assemblages increased, but not during the following decade, when the North Sea warmed (Figures 3d,e vs. 6d).
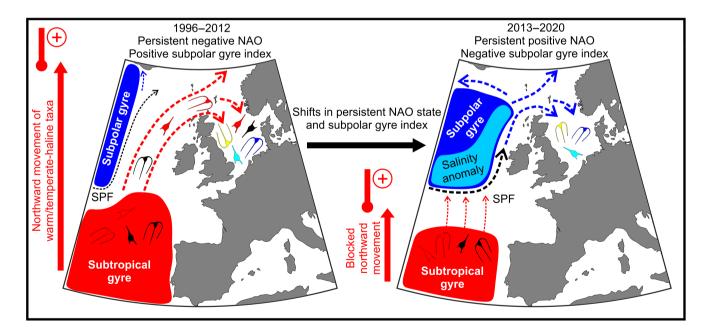

FIGURE 7 Schematics illustrating how hydro-climatic variability and oceanic circulation affected the biodiversity of North Sea dinoflagellates between 1996 and 2020. Left and right panels represent the situations observed between 1996 and 2012 (persistent negative North Atlantic Oscillation [NAO] phase and positive subpolar gyre index) and 2013–2020 (persistent positive NAO phase and negative subpolar gyre index), respectively. In each panel, red and dark blue areas display the position and spatial expansion of the subtropical and subpolar gyres, respectively. Pale blue area in the right panel displays the position of the salinity anomaly observed in the eastern subpolar Northeast Atlantic after 2012. Dashed red and blue arrows exhibit the positions of the main currents originating from the subtropical and subpolar gyres, respectively. Black dashed arrows display the position of the subpolar front (SPF). Arrow width is proportional to the supposed current flow and speed. Red bold arrow on the left of each schematic represents the northward movement of the warm/temperate-haline assemblages in response to increasing temperature (i.e. climate warming). Dinoflagellate colour enables the distinction of the five assemblages identified by means of the cluster analysis (see Figure 2 legend).

4 | DISCUSSION AND CONCLUSION

Our results indicate that shifts in dinoflagellate biomass and biodiversity have resulted from the interaction between increasing temperature and natural hydro-climatic variability that affect large-scale and regional oceanic circulation (e.g. subpolar gyre and oceanic inflow into the North Sea). More precisely, from 1958 to 2012, ocean warming enabled the northward movement of warm/temperate-haline taxa along the European Shelf-edge (Figures 5–7; Figure S8) and their subsequent advection into the North Sea via the North Atlantic Current. This phenomenon was amplified between 1996 and 2012 by the westward contraction of the subpolar gyre and by the mid-1990s shifts in NAO and AMO states, which were associated with an enhanced warming and the northward advection of subtropical waters along the European shelf-edge (Figures 6 and 7) (Reid et al., 2001). Similar results were observed in the Barents Sea, where increased advection of southern waters rather than temperature has been identified as the main mechanism explaining the spatio-temporal expansion of more temperate taxa (Oziel et al., 2020). However, the temperature must remain suitable to enable the survival of the advected taxa in a given region because ectotherms are sensitive to small changes in temperature (i.e. they better tolerate cooling than warming) (Martin & Huey, 2008; Thomas et al., 2012).

The strong reduction in biodiversity and biomass observed during the mid-2010s paralleled an exceptional freshening and cooling of the Northeast Atlantic (Desbruyères et al., 2021; Holliday et al., 2020; Josey et al., 2018) (Figures S10 and S11), associated with an eastward expansion of the subpolar gyre. This event was accompanied by a positive persistent NAO (i.e. more westerly winds, Hurrell & Deser, 2010), which reinforced the transport of subpolar waters into the Rockall Trough and further along the European shelf-edge via the slope current (Figure 7) (Marsh et al., 2017), causing negative salinity and temperature anomalies in the North Sea circa 2010 (Figure 6d; Figures S10 and S11). A stronger oceanic inflow was also observed at that time, which may have facilitated the entry of subpolar waters into the North Sea and therefore explained the increase in biomass of the temperate hypohaline and psychrophilous assemblages. However, shortly after 2010, the North Sea temperature started to rise, while the biomass of the temperate hypohaline and psychrophilous assemblages were declining. As the salinity of the waters entering through the north-west North Sea was low (Figure S9e) and the subpolar gyre was still in an eastward expansion, subpolar waters were still dominating the oceanic inflow (Figure 6a) (Hátún et al., 2005; Koul et al., 2019). Therefore, it indicates a warming of those waters when reaching the North Sea (contrary to temperature, salinity is approximately conserved within water masses) (Curry & Mauritzen, 2005). Hence, it is very likely that North Sea warming caused the decline in biomass of the temperate hypohaline and psychrophylous assemblage, (which should have been favoured by the advection of subpolar waters) an hypothesis that is reinforced by the phenological shifts exhibited by those assemblages (Figures 3n,o and 4; Figures S5–S7), which correspond with theoretical expectations of taxa responding to climate warming (i.e. summer taxa, as the temperate and temperate hypohaline assemblage, are expected to exhibit an earlier phenology, while taxa at the southern edge of their distributional range, as the psychrophylous assemblage, are expected to decline) (Beaugrand & Kirby, 2018). Furthermore, those assemblages account for the largest part of the total North Sea dinoflagellate biomass, and warming has already been identified as a main driver of their decline in this area (Hinder et al., 2012).

On the contrary, it is very unlikely that the observed decline in salinity altered the physiology of the warm and temperate-haline groups and caused their collapse (Brand, 1984). Hence, this event might be more likely related to the shift in the strength of the subpolar gyre and the associated location of the subpolar front (i.e. eastward shift) and the strong salinity anomaly that crossed the North Atlantic, which may have blocked the northward advection of those assemblages (Figure 7) (Holliday et al., 2020; Vecchione et al., 2015). This hypothesis implies that the warm/temperate-haline assemblages were not self-sustained in the North Sea and have been continuously advected in this area during the last decades. Therefore, the decline of North Sea dinoflagellates may continue, unless changes in the strength of the subpolar gyre enable once again an advection and a maintenance of the warm/temperate-haline taxa. Hence, it is the combined effect of both warming and changes in oceanic circulation that conspired together to alter North Sea dinoflagellate biodiversity and biomass. (The presence of deeper living taxa, such as *Ceratium. praelongum* and *C. platycorne* (Sournia, 1982), can also be indicative of the effect of water mixing).

In conclusion, as ocean temperature rises, species distributions are generally expected to track towards historically cooler regions in line with their thermal affinities (Thomas et al., 2012). However, our study shows that this is not fully the case for dinoflagellates and that a warming North Atlantic will not result in populations simply adjusting their distributions northward to align with shifting thermal isotherms. Furthermore, phytoplankton are usually assimilated to passive drifters and therefore have to be advected by currents in regions where the environmental conditions allow their survival. Hence, hydro-climatic variability in oceanic currents should also be considered to project future phytoplankton changes.

AUTHOR CONTRIBUTIONS

Loïck Kléparski: Conceptualization; data curation; formal analysis; funding acquisition; investigation; methodology; software; validation; visualization; writing – original draft; writing – review and editing. **Grégory Beaugrand:** Conceptualization; data curation; formal analysis; funding acquisition; investigation; methodology; software; supervision; visualization; writing – original draft; writing – review and editing. **Clare Ostle:** Conceptualization; methodology; writing – original draft; writing – review and editing. **Martin Edwards:** Conceptualization; methodology; writing – original draft; writing – review and editing. **Morten D. Skogen:** Conceptualization; methodology; writing – original draft; writing – review and editing. **Nicolas Djeghri:** Conceptualization; methodology; writing – original draft; writing – review and editing. **Hjálmar

CONFLICT OF INTEREST STATEMENT

The authors declare no conflict of interest.

DATA AVAILABILITY STATEMENT

All the data used in this article are already freely available (see Section 2; Text S1).

ORCID

Loïck Kléparski https://orcid.org/0000-0002-7536-2941
Grégory Beaugrand https://orcid.org/0000-0002-0712-5223
Clare Ostle https://orcid.org/0000-0001-6923-5535
Martin Edwards https://orcid.org/0000-0002-5716-4714
Morten D. Skogen https://orcid.org/0000-0002-6304-7282
Nicolas Djeghri https://orcid.org/0000-0001-5740-3386
Hjálmar Hátún https://orcid.org/0000-0002-9312-7355

REFERENCES

Barton, A. D., Finkel, Z. V., Ward, B. A., Johns, D. G., & Follows, M. J. (2013). On the roles of cell size and trophic strategy in North Atlantic diatom and dinoflagellate communities. *Limnology and Oceanography, 58*(1), 254–266. https://doi.org/10.4319/lo.2013.58.1.0254

Batten, S. D., Clark, R., Flinkman, J., Hays, G., John, E., John, A. W. G., Jonas, T., Lindley, J. A., Stevens, D. P., & Walne, A. (2003). CPR sampling: The technical background, materials and methods, consistency and comparability. *Progress in Oceanography, 58*(2–4), 193–215. https://doi.org/10.1016/j.pocean.2003.08.004

Beaugrand, G. (2004). The North Sea regime shift: Evidence, causes, mechanisms and consequences. *Progress in Oceanography, 60*(2–4), 245–262. https://doi.org/10.1016/j.pocean.2004.02.018

Beaugrand, G., Faillettaz, R., & Kirby, R. R. (2021). Absence of an internal multidecadal oscillation in the North Atlantic has consequences for anticipating the future of marine ecosystems. *Climate Research, 85*, 107–111. https://doi.org/10.3354/cr01676

Beaugrand, G., Harlay, X., & Edwards, M. (2014). Detecting plankton shifts in the North Sea: A new abrupt ecosystem shift between 1996 and 2003. *Marine Ecology Progress Series, 502*, 85–104. https://doi.org/10.3354/meps10693

Beaugrand, G., & Kirby, R. R. (2018). How do marine pelagic species respond to climate change? Theories and observations. *Annual Review of Marine Science, 10*(1), 169–197. https://doi.org/10.1146/annurev-marine-121916-063304

Beaugrand, G., & Reid, P. C. (2012). Relationships between North Atlantic salmon, plankton, and hydroclimatic change in the Northeast Atlantic. *ICES Journal of Marine Science, 69*(9), 1549–1562. https://doi.org/10.1093/icesjms/fss153

Brand, L. E. (1984). The salinity tolerance of forty-six marine phytoplankton isolates. *Estuarine, Coastal and Shelf Science, 18*, 543–556. https://doi.org/10.1016/0272-7714(84)90089-1

Brown, J. H. (1984). On the relationship between abundance and distribution of species. *The American Naturalist, 124*(2), 255–279. https://doi.org/10.1086/284267

Chivers, W. J., Edwards, M., & Hays, G. C. (2020). Phenological shuffling of major marine phytoplankton groups over the last six decades. *Diversity and Distributions, 26*(5), 536–548. https://doi.org/10.1111/ddi.13028

Curry, R., & Mauritzen, C. (2005). Dilution of the northern North Atlantic Ocean in recent decades. *Science, 308*(5729), 1772–1774. https://doi.org/10.1126/science.1109477

Desbruyères, D., Chafik, L., & Maze, G. (2021). A shift in the ocean circulation has warmed the subpolar North Atlantic Ocean since 2016. *Communications Earth & Environment, 2*(1), 48. https://doi.org/10.1038/s43247-021-00120-y

Dickson, R. R., Meincke, J., Malmberg, S. A., & Lee, A. L. (1988). The "great salinity anomaly" in the northern North Atlantic 1968–1982. *Progress in Oceanography, 20*(2), 103–151. https://doi.org/10.1016/0079-6611(88)90049-3

Djeghri, N., Boyé, A., Ostle, C., & Hélaouët, P. (2023). Reinterpreting two regime shifts in North Sea plankton communities through the lens of functional traits. *Global Ecology and Biogeography, 32*, 962–975. https://doi.org/10.1111/geb.13659

Edwards, M., Beaugrand, G., Helaouët, P., Alheit, J., & Coombs, S. (2013). Marine ecosystem response to the Atlantic Multidecadal Oscillation. *PLoS One, 8*(2), e57212. https://doi.org/10.1371/journal.pone.0057212

Edwards, M., Beaugrand, G., Kléparski, L., Helaouët, P., & Reid, P. C. (2022). Climate variability and multi-decadal diatom abundance in the Northeast Atlantic. *Communications Earth & Environment, 3*, 162. https://doi.org/10.1038/s43247-022-00492-9

Edwards, M., Beaugrand, G., Reid, P. C., Rowden, A. A., & Jones, M. B. (2002). Ocean climate anomalies and the ecology of the North Sea. *Marine Ecology Progress Series, 239*, 1–10. https://doi.org/10.3354/meps239001

Edwards, M., Reid, P. C., & Planque, B. (2001). Long-term and regional variability of phytoplankton biomass in the Northeast Atlantic (1960–1995). *ICES Journal of Marine Science, 58*, 39–49. https://doi.org/10.1006/jmsc.2000.0987

Faillettaz, R., Beaugrand, G., Goberville, E., & Kirby, R. R. (2019). Atlantic Multidecadal Oscillations drive the basin-scale distribution of Atlantic bluefin tuna. *Science Advances*, *5*(1), eaar6993. https://doi.org/10.1126/sciadv.aar6993

Fehling, J., Davidson, K., Bolch, C. J. S., Brand, T. D., & Narayanaswamy, B. E. (2012). The relationship between phytoplankton distribution and water column characteristics in north west European Shelf Sea waters. *PLoS One*, *7*(3), e34098. https://doi.org/10.1371/journal.pone.0034098

Gao, S., Hjøllo, S. S., Falkenhaug, T., Strand, E., Edwards, M., & Skogen, M. D. (2021). Overwintering distribution, inflow patterns and sustainability of *Calanus finmarchicus* in the North Sea. *Progress in Oceanography*, *194*, 102567. https://doi.org/10.1016/j.pocean.2021.102567

Hátún, H., & Chafik, L. (2018). On the recent ambiguity of the North Atlantic subpolar gyre index. *Journal of Geophysical Research: Oceans*, *123*(8), 5072–5076. https://doi.org/10.1029/2018JC014101

Hátún, H., Payne, M. R., Beaugrand, G., Reid, P. C., Sandø, A. B., Drange, H., Hansen, B., Jacobsen, J. A., & Bloch, D. (2009). Large biogeographical shifts in the north-eastern Atlantic Ocean: From the subpolar gyre, via plankton, to blue whiting and pilot whales. *Progress in Oceanography*, *80*(3–4), 149–162. https://doi.org/10.1016/j.pocean.2009.03.001

Hátún, H., Sandø, A. B., Drange, H., Hansen, B., & Valdimarsson, H. (2005). Influence of the Atlantic subpolar gyre on the thermohaline circulation. *Science*, *309*(5742), 1841–1844. https://doi.org/10.1126/science.1114777

Hinder, S. L., Hays, G. C., Edwards, M., Roberts, E. C., Walne, A. W., & Gravenor, M. B. (2012). Changes in marine dinoflagellate and diatom abundance under climate change. *Nature Climate Change*, *2*(4), 271–275. https://doi.org/10.1038/nclimate1388

Hjøllo, S. S., Skogen, M. D., & Svendsen, E. (2009). Exploring currents and heat within the North Sea using a numerical model. *Journal of Marine Systems*, *78*, 180–192.

Holliday, N. P., Bersch, M., Berx, B., Chafik, L., Cunningham, S., Florindo-López, C., Hátún, H., Johns, W., Josey, S. A., Larsen, K. M., Mulet, S., Oltmanns, M., Reverdin, G., Rossby, T., Thierry, V., Valdimarsson, H., & Yashayaev, I. (2020). Ocean circulation causes the largest freshening event for 120 years in eastern subpolar North Atlantic. *Nature Communications*, *11*(1), 585. https://doi.org/10.1038/s41467-020-14474-y

Hurrell, J. W., & Deser, C. (2010). North Atlantic climate variability: The role of the North Atlantic Oscillation. *Journal of Marine Systems*, *79*, 231–244. https://doi.org/10.1016/j.jmarsys.2009.11.002

Hutchinson, G. E. (1957). Concluding remarks. *Cold Spring Harbor Symposia on Quantitative Biology*, *22*, 415–427.

IPCC. (2019). Technical summary. In D. C. Roberts, H. O. Pörtner, V. Masson-Delmotte, P. Zhai, E. Poloczanska, K. Mintenbeck, M. Tignor, A. Alegria, M. Nicolai, A. Okem, J. Petzold, B. Rama, & N. M. Weyer (Eds.), *IPCC special report on the ocean and cryosphere in a changing climate* (pp. 39–69). Cambridge University Press.

Jonas, T. D., Walne, A. W., Beaugrand, G., Gregory, L., & Hays, G. C. (2004). The volume of water filtered by a Continuous Plankton Recorder sample: The effect of ship speed. *Journal of Plankton Research*, *26*(12), 1499–1506. https://doi.org/10.1093/plankt/fbh137

Josey, S. A., Hirschi, J. J. M., Sinha, B., Duchez, A., Grist, J. P., & Marsh, R. (2018). The recent Atlantic cold anomaly: Causes, consequences, and related phenomena. *Annual Review of Marine Science*, *10*(1), 475–501. https://doi.org/10.1146/annurev-marine-121916-063102

Kemp, A. E. S., & Villareal, T. A. (2018). The case of the diatoms and the muddled mandalas: Time to recognize diatom adaptations to stratified waters. *Progress in Oceanography*, *167*, 138–149. https://doi.org/10.1016/j.pocean.2018.08.002

Kléparski, L., & Beaugrand, G. (2022). The species chromatogram, a new graphical method to represent, characterise and compare the ecological niches of different species. *Ecology and Evolution*, *12*(4), e8830. https://doi.org/10.1002/ece3.8830

Koul, V., Schrum, C., Düsterhus, A., & Baehr, J. (2019). Atlantic inflow to the North Sea modulated by the subpolar gyre in a historical simulation with MPI-ESM. *Journal of Geophysical Research: Oceans*, *124*(3), 1807–1826. https://doi.org/10.1029/2018JC014738

Legendre, P., & Legendre, L. (1998). *Numerical Ecology*. Elsevier.

Leterme, S. C., Pingree, R. D., Skogen, M., Seuront, L., Reid, P. C., & Attrill, M. J. (2008). Decadal fluctuations in North Atlantic water inflow in the North Sea between 1958–2003: Impact on temperature and phytoplankton populations. *Oceanologia*, *50*(1), 59–72.

Lewandowska, A., & Sommer, U. (2010). Climate change and the spring bloom: A mesocosm study on the influence of light and temperature on phytoplankton and mesozooplankton. *Marine Ecology Progress Series*, *405*, 101–111. https://doi.org/10.3354/meps08520

Ligowski, R., Jordan, R. W., & Assmy, P. (2012). Morphological adaptation of a planktonic diatom to growth in Antarctic sea ice. *Marine Biology*, *159*(4), 817–827.

Luczak, C., Beaugrand, G., Jaffré, M., & Lenoir, S. (2011). Climate change impact on Balearic shearwater through a trophic cascade. *Biology Letters*, *7*(5), 702–705. https://doi.org/10.1098/rsbl.2011.0225

Malviya, S., Scalco, E., Audic, S., Vincent, F., Veluchamy, A., Poulain, J., Wincker, P., Iudicone, D., de Vargas, C., Bittner, L., Zingone, A., & Bowler, C. (2016). Insights into global diatom distribution and diversity in the world's ocean. *Proceedings of the National Academy of Sciences of the United States of America*, *113*(11), 1516–1525. https://doi.org/10.1073/pnas.1509523113

Mann, M. E., Steinman, B. A., Brouillette, D. J., & Miller, S. K. (2021). Multidecadal climate oscillations during the past millennium driven by volcanic forcing. *Science*, *371*(6533), 1014–1019. https://doi.org/10.1126/science.abc5810

Margalef, R. (1978). Life-forms of phytoplankton as survival alternatives in an unstable environment. *Oceanologica Acta*, *1*(4), 493–509.

Marsh, R., Haigh, I. D., Cunningham, S. A., Inall, M. E., Porter, M., & Moat, B. I. (2017). Large-scale forcing of the European slope current and associated inflows to the North Sea. *Ocean Science*, *13*(2), 315–335. https://doi.org/10.5194/os-13-315-2017

Martin, T. L., & Huey, R. B. (2008). Why "suboptimal" is optimal: Jensen's inequality and ectotherm thermal preferences. *The American Naturalist*, *171*(3), E102–E118. https://doi.org/10.1086/527502

Oziel, L., Baudena, A., Ardyna, M., Massicotte, P., Randelhoff, A., Sallée, J. B., Ingvaldsen, R. B., Devred, E., & Babin, M. (2020). Faster Atlantic currents drive poleward expansion of temperate phytoplankton in the Arctic Ocean. *Nature Communications*, *11*, 1705. https://doi.org/10.1038/s41467-020-15485-5

Reid, P. C., Edwards, M., Beaugrand, G., Skogen, M., & Stevens, D. (2003). Periodic changes in the zooplankton of the North Sea during the twentieth century linked to oceanic inflow: Calanus and oceanic inflow to the North Sea. *Fisheries Oceanography*, *12*(4–5), 260–269. https://doi.org/10.1046/j.1365-2419.2003.00252.x

Reid, P. C., Holliday, N. P., & Smyth, T. J. (2001). Pulses in the eastern margin current and warmer water off the north west European shelf linked to North Sea ecosystem changes. *Marine Ecology Progress Series*, *215*, 283–287. https://doi.org/10.3354/meps215283

Richardson, A. J., Walne, A. W., John, A. W. G., Jonas, T. D., Lindley, J. A., Sims, D. W., Stevens, D., & Witt, M. (2006). Using Continuous Plankton Recorder data. *Progress in Oceanography*, *68*(1), 27–74. https://doi.org/10.1016/j.pocean.2005.09.011

Righetti, D., Vogt, M., Gruber, N., Psomas, A., & Zimmermann, N. E. (2019). Global pattern of phytoplankton diversity driven by temperature and environmental variability. *Science Advances*, *5*(5), eaau6253. https://doi.org/10.1126/sciadv.aau6253

Smayda, T. J., & Reynolds, C. S. (2003). Strategies of marine dinoflagellate survival and some rules of assembly. *Journal of Sea Research*, *49*(2), 95–106. https://doi.org/10.1016/S1385-1101(02)00219-8

Sournia, A. (1982). Is there a shade flora in the marine plankton? *Journal of Plankton Research*, *4*(2), 391–399. https://doi.org/10.1093/plankt/4.2.391

Thomas, M. K., Kremer, C. T., Klausmeier, C. A., & Litchman, E. (2012). A global pattern of thermal adaptation in marine phytoplankton. *Science*, *338*(6110), 1085–1088. https://doi.org/10.1126/science.1224836

Tréguer, P., Bowler, C., Moriceau, B., Dutkiewicz, S., Gehlen, M., Aumont, O., Bittner, L., Dugdale, R., Finkel, Z., Iudicone, D., Jahn, O., Guidi, L., Lasbleiz, M., Leblanc, K., Levy, M., & Pondaven, P. (2018). Influence of diatom diversity on the ocean biological carbon pump. *Nature Geoscience*, *11*(1), 27–37. https://doi.org/10.1038/s41561-017-0028-x

Vecchione, M., Falkenhaug, T., Sutton, T., Cook, A., Gislason, A., Hansen, H. Ø., Heino, M., Miller, P. I., Piatkowski, U., Porteiro, F., Søiland, H., & Bergstad, O. A. (2015). The effect of the North Atlantic sub-polar front as a boundary in pelagic biogeography decreases with increasing depth and organism size. *Progress in Oceanography*, *138*, 105–115. https://doi.org/10.1016/j.pocean.2015.08.006

Warner, A. J., & Hays, G. C. (1994). Sampling by the Continuous Plankton Recorder survey. *Progress in Oceanography*, *34*(2–3), 237–256. https://doi.org/10.1016/0079-6611(94)90011-6

SUPPORTING INFORMATION

Additional supporting information can be found online in the Supporting Information section at the end of this article.

How to cite this article: Kléparski, L., Beaugrand, G., Ostle, C., Edwards, M., Skogen, M. D., Djeghri, N., & Hátún, H. (2024). Ocean climate and hydrodynamics drive decadal shifts in Northeast Atlantic dinoflagellates. *Global Change Biology*, *30*, e17163. https://doi.org/10.1111/gcb.17163